Jahn-Teller distortion in the lowest excited singlet state of C_{60}

Shugo Suzuki, Daisuke Inomata, Naoya Sashide, and Kenji Nakao
Institute of Materials Science, University of Tsukuba, Tsukuba 305, Japan
(Received 13 July 1993)

Several properties of the lowest excited singlet state of the C_{60} molecule are investigated with reference to the Jahn-Teller distortion. We find that the symmetry of the molecular structure in the relaxed excited state is approximately the C_{2h} symmetry, though the strict symmetry is that of the inversion group C_i. Also it is found that the most remarkable contribution to the Jahn-Teller distortion is given by the h_g mode of the lowest frequency and the next by the h_g mode of the fourth-lowest frequency. Furthermore, we calculate the frequencies of the normal modes in the relaxed excited state. It is shown that the frequency splittings of the h_g modes of the lowest and the fourth-lowest frequency reach several tens of cm^{-1}. Also it is pointed out that the two h_g modes are the radial and the tangential mode described by the second-order vector spherical harmonics.

I. INTRODUCTION

The optical response of the fullerene C_{60} is one of the most appealing subjects of this new material with reference to applications to optical devices utilizing photoconduction,[1,2] optical nonlinearity,[3,4] etc. Since the properties of electronically excited states are important to explain optical phenomena, the nature of the excited states of C_{60} is being intensely studied, also especially by means of the measurements of optical absorption[5–10] and photoluminescence spectra.[11–15]

The absorption spectra show a weak and broad band in the visible region and several strong bands in the ultraviolet region. The general appearance of the spectra is well explained by the results of the quantum chemical calculations;[16–19] the weak and broad band extending from 1.9 to 2.8 eV is composed of orbitally forbidden transitions from the ^1A_g ground state to the low-lying excited states, $^1T_{1g}$, $^1T_{2g}$, and ^1G_g, while the strong bands observed above 3 eV are assigned to the allowed transitions to certain $^1T_{1u}$ states.

Recently, a well-resolved fluorescence spectrum has been observed from C_{60} in methylcyclohexane.[14] Moreover, almost the same spectrum from a thin film of C_{60} is observed;[15] both of the fluorescence bands with a peak at 1.7 eV show broad widths and extend from the absorption edge (1.9 eV) to the infrared region, accompanied by a shoulder at 1.5 eV. This band is assigned to an orbitally forbidden transition from the lowest excited singlet state to the ground state. The absorption and the fluorescence spectra, however, exhibit complicated vibrational structures. In particular, this is remarkable for the broad bands relating to the low-lying excited states. Such vibrational structures imply the significance of the electron-phonon interaction in the low-lying excited states. Although several interpretations of such vibrational structures are proposed, a decent explanation has not been established.[10,19]

Furthermore, it is suggested that the fluorescence spectrum observed from the film of C_{60} originates from self-trapped polaron excitons.[15] The self-trapping also indicates substantial coupling of the electronically excited states with the deformation of the C_{60} molecule. Actually, it is most likely that the low-lying excited states are extensively subjected to the Jahn-Teller distortion because these states are almost degenerate within the energy interval of $\sim$0.1 eV.[16–19] Also, it is well known that the relaxation of the excited state usually affects the optical spectra considerably. Therefore, it is important to elucidate the properties of the lowest excited state with respect to the Jahn-Teller distortion in order to explain the characteristics of the optical spectra. Nevertheless, there are few studies on the Jahn-Teller distortion in the low-lying excited states.

The purpose of the present paper is to investigate the properties of the lowest excited singlet state of C_{60} with reference to the Jahn-Teller distortion. By using a model Hamiltonian that describes the interaction between the low-lying excited states and the intramolecular vibrations, we elucidate the vibrational modes significantly contributing to the Jahn-Teller distortion. Furthermore, we calculate the eigenfrequencies of the intramolecular vibrations in the relaxed excited state. In Sec. II, the method of calculations is described. Section III is devoted to results and discussion. Conclusions are given in Sec. IV.

II. METHOD OF CALCULATION

A. Low-lying excited states

The full symmetry of the C_{60} molecule is that of the icosahedral point group I_h, so that the irreducible representations of I_h are available for the classification of the molecular orbitals and the normal modes. The highest occupied molecular orbitals (HOMO) and the lowest unoccupied molecular orbitals (LUMO), of the C_{60} molecule are fivefold-degenerate h_u and threefold-degenerate t_{1u} orbitals, respectively. Consequently, by transferring an electron from HOMO to LUMO, there arise 15 excited singlet states of even parity. The singlet state where an electron is removed from HOMO a and is added to LUMO m is denoted by $|ma\rangle$:

$$|ma\rangle = \frac{1}{\sqrt{2}}(\phi^{\dagger}_{m\uparrow}\phi_{a\uparrow} + \phi^{\dagger}_{m\downarrow}\phi_{a\downarrow})|^1A_g\rangle \ , \tag{1}$$

where $m = 1, 2, 3$ and $a = 1, 2, 3, 4, 5$. Also $\phi^{\dagger}_{m\sigma}$ and $\phi_{a\sigma}$ are the creation operator for the σ-spin electron in LUMO m and the annihilation operator for that in HOMO a, respectively. In the present study, we restrict ourselves to the description of the low-lying excited states in terms of the linear combinations of the 15 states $|ma\rangle$.

Furthermore, the excited states, $^1T_{1g}$, $^1T_{2g}$, ^1G_g, and ^1H_g, are derived from $|ma\rangle$, i.e., $h_u \times t_{1u} = T_{1g} + T_{2g} + G_g + H_g$; in fact, the energy levels of these states split due to the electron correlation.[16–19] In the present study, we use the states, $^1T_{1g}$, $^1T_{2g}$, ^1G_g, and ^1H_g, as the new basis; the Ith state belonging to the Γ level is denoted by $|\Gamma I\rangle$ where Γ is a label for T_{1g}, T_{2g}, G_g, or H_g. The transformation of the basis from $|ma\rangle$ to $|\Gamma I\rangle$ is performed by using the projection operators of the I_h group. It should be noted that $|\Gamma I\rangle$ are uniquely determined by the projection operators without normalization constants because each Γ appears only once in $h_u \times t_{1u}$. The projection operator that extracts $|\Gamma I\rangle$ is given by

$$P^{(\Gamma)}_I = \frac{d_\Gamma}{120}\sum_G D^{(\Gamma)}_{II'}(G)^* G \ , \tag{2}$$

where $D^{(\Gamma)}_{II'}(G)$ is the I, I'th element of the Γ representation of the group element G and d_Γ is the dimension of Γ. Then $|\Gamma I\rangle$ is obtained by operating $P^{(\Gamma)}_I$ on a certain state $|ma\rangle$. Finally, one finds

$$|\Gamma I\rangle = \sum_{ma} C^{\Gamma I}_{ma}|ma\rangle \ , \tag{3}$$

where

$$C^{\Gamma I}_{ma} \propto \frac{d_\Gamma}{120}\sum_G D^{(\Gamma)}_{II'}(G)^* D^{(T_{1u})}_{mm'}(G) D^{(H_u)}_{aa'}(G)^* \ . \tag{4}$$

Here we choose $C^{\Gamma I}_{ma}$ so as to normalize $|\Gamma I\rangle$. In the derivation of the above results, we use the following:

$$G\phi^{\dagger}_{m\uparrow}\phi_{a\uparrow}|^1A_g\rangle = G\phi^{\dagger}_{m\uparrow}G^{\dagger}G\phi_{a\uparrow}G^{\dagger}|^1A_g\rangle \ , \tag{5}$$

and

$$\begin{aligned} G\phi^{\dagger}_{m\uparrow}G^{\dagger} &= \sum_{m'}\phi^{\dagger}_{m'\uparrow}D^{(T_{1u})}_{m'm}(G) \ , \\ G\phi_{a\uparrow}G^{\dagger} &= \sum_{a'}\phi_{a'\uparrow}D^{(H_u)}_{a'a}(G)^* \ . \end{aligned} \tag{6}$$

In Eq. (5), we adopt the fact that the ^1A_g state is symmetrical under all group operations, i.e., $G|^1A_g\rangle = |^1A_g\rangle$. We also use the relations corresponding to Eqs. (5) and (6) for the term $\phi^{\dagger}_{m\downarrow}\phi_{a\downarrow}|^1A_g\rangle$ in Eq. (1).

B. Electron-phonon interaction

Individual electrons are subjected to the screened attractive potential due to the sixty carbon nuclei. We write this in the following form:

$$V(\mathbf{r}) = -\frac{Ze^2}{\epsilon}\sum_{k=1}^{60}\frac{1}{|\mathbf{r} - \mathbf{R}_k|} \ , \tag{7}$$

where $Z(= 6)$ is the atomic number of carbon and ϵ is the dielectric constant. It is natural to consider that the dielectric constant ϵ is that of the far infrared frequency, because the order of the period of the nuclear motion is $\sim 10^{-12}$ s. It is appropriate, however, to exploit the static dielectric constant because of the nonpolarity of C_{60}; we assume $\epsilon = 6$ in the present study, referring to the dielectric constant of diamond ($\epsilon = 5.93$).

By expanding $V(\mathbf{r})$ with respect to the displacement $\mathbf{u}_k$ of the kth carbon atom from its equilibrium position $\mathbf{R}^0_k$ ($\mathbf{R}_k = \mathbf{R}^0_k + \mathbf{u}_k$), one finds the electron-phonon interaction, $V^{\rm ep}(\mathbf{r}, u)$, where we denote the whole of the displacements $\{\mathbf{u}_k | k = 1, \ldots, 60\}$ by u:

$$V(\mathbf{r}) = -\frac{Ze^2}{\epsilon}\sum_{k=1}^{60}\frac{1}{|\mathbf{r} - \mathbf{R}^0_k|} + V^{\rm ep}(\mathbf{r}, u) \ . \tag{8}$$

Here

$$V^{\rm ep}(\mathbf{r}, u) = -\frac{Ze^2}{\epsilon}\sum_{k=1}^{60}\frac{\mathbf{u}_k \cdot (\mathbf{r} - \mathbf{R}^0_k)}{|\mathbf{r} - \mathbf{R}^0_k|^3} \ . \tag{9}$$

Therefore, the one-electron matrix elements between the molecular orbitals are given by

$$V^{\rm ep}_{ij}(u) = \int d\mathbf{r}\, \phi_i(\mathbf{r})^* V^{\rm ep}(\mathbf{r}, u)\phi_j(\mathbf{r}) \ , \tag{10}$$

where $\phi_i(\mathbf{r})$ and $\phi_j(\mathbf{r})$ are the one-electron wave function of the molecular orbital i and that of the molecular orbital j, respectively.

Furthermore, the matrix element of the electron-phonon interaction between $|ma\rangle$ and $|m'a'\rangle$ is given by[20]

$$H^{\rm ep}_{ma,m'a'}(u) = V^{\rm ep}_{mm'}(u)\delta_{aa'} - V^{\rm ep}_{aa'}(u)\delta_{mm'} \ , \tag{11}$$

where the negative sign of the second term in the right-hand side of Eq. (11) is due to the removal of an electron from HOMO. As a result, we obtain the matrix element of the electron-phonon interaction between $|\Gamma I\rangle$ and $|\Gamma' I'\rangle$:

$$H^{\rm ep}_{\Gamma I,\Gamma' I'}(u) = \sum_{ma,m'a'} C^{\Gamma I *}_{ma} C^{\Gamma' I'}_{m'a'} H^{\rm ep}_{ma,m'a'}(u) \ . \tag{12}$$

In order to obtain $H^{\rm ep}_{\Gamma I,\Gamma' I'}(u)$, it is necessary to calculate $V^{\rm ep}_{ij}(u)$ defined in Eq. (10). For this purpose, we carry out the first-principle calculation of the electronic ground state of C_{60}, adopting the same method employed by Disch and Schulman,[21] i.e., the self-consistent calculation by the Hartree-Fock method with the minimal basis set; the calculation is performed by using the observed values of the single-bond length (1.46 Å) and the double-bond length (1.40 Å).[22] Then the resultant one-electron wave functions, $\phi_i(\mathbf{r})$ and $\phi_j(\mathbf{r})$, are exploited to calculate $V^{\rm ep}_{ij}(u)$.

C. Normal modes in the ground state

We now describe the method to represent the intramolecular vibrations of C_{60}. In the present study, it

TABLE I. The force constants of the stretching springs (K_{str}), in eV/Å^2, and of the bending springs (K_{bend}), in eV/rad^2.

K_{str}	Value	K_{bend}	Value
k_{s1}	12.03	k_{b5}	5.07
k_{s2}	24.26	k_{b6}	11.08
k_{s11}	4.58		
k_{s12}	6.71		

is assumed that the vibrational properties are described by the force-constant model. That is, the elastic energy, $E_{elastic}(u)$, due to the deformation of the molecule is assumed as

$$E_{elastic}(u) = \frac{1}{2}\sum_{\alpha,\beta=1}^{180} u_\alpha k_{\alpha\beta} u_\beta \ . \tag{13}$$

Here u_α and u_β are the components of the displacements of the sixty carbon nuclei from their equilibrium positions and $k_{\alpha\beta}$ represent the elements of the force-constant matrix. Then one can obtain the eigenfrequency of the γ mode, ω_γ, by diagonalizing the force-constant matrix $k_{\alpha\beta}$. That is,

$$E_{elastic}(u) = \frac{1}{2}\sum_{\gamma,i} m\omega_\gamma^2 Q_{\gamma i}^2 \ , \tag{14}$$

where m is the mass of a carbon atom and $Q_{\gamma i}$ is the ith normal coordinate of the γ mode. In the present study, we employ the stretching and the bending springs explained below in order to obtain the specific expressions of $k_{\alpha\beta}$.

The stretching springs between the carbon atoms cause the recovery forces acting on them, i.e., the forces come from the deviations from the equilibrium distances between two atoms connected by the springs. In our model, we employ the springs which describe the stretching motions of the single bonds in the pentagons and the double bonds in the hexagons; the force constant of the single-bond springs is denoted by k_{s1} and that of the double-bond springs by k_{s2}. Furthermore, we use the springs between the next nearest-neighbor atoms in the pentagons and those in the hexagons; the force constant of the former is denoted by k_{s11} and that of the latter by k_{s12}.

Also the bending springs are assumed between the nearest-neighbor bonds; the bending springs describe the recovery forces arising from the deviations from the equilibrium angles between the bonds. We use two kinds of bending springs; one corresponds to the springs between the nearest-neighbor bonds in the pentagons and the other to those in the hexagons. We denote the force constant of the former and that of the latter by k_{b5} and k_{b6}, respectively.

In Table I, we list the values of the force constants determined so as to reproduce the frequencies of the normal modes observed in the Raman scattering spectroscopy[23] (two a_g and eight h_g modes) and those observed in the infrared absorption spectroscopy[24] (four t_{1u} modes). The observed and the calculated frequencies are given in Table II; the average error is found to be ~4%.

D. Model Hamiltonian

In the present study, we investigate the Jahn-Teller distortion in the lowest excited state by applying the following Hamiltonian:

$$H = \sum_{\Gamma I,\Gamma' I'} |\Gamma I\rangle [E_\Gamma \delta_{\Gamma I,\Gamma' I'} + H^{ep}_{\Gamma I,\Gamma' I'}(u)] \langle \Gamma' I'| + E_{elastic}(u) \ . \tag{15}$$

Here we adopt the adiabatic approximation, i.e., the kinetic energies of the carbon nuclei are ignored. Also E_Γ is the energy of the Γ level measured from the energy of the ^1A_g ground state and $H^{ep}_{\Gamma I,\Gamma' I'}(u)$ are the matrix elements of the electron-phonon interaction explained in Sec. II B. Furthermore, the last term represents the elastic energy due to the deformation of the C_{60} molecule expressed by the force-constant model described in Sec. II C.

We use E_Γ which have been estimated by the quantum chemical calculations taking account of a configuration interaction; E_Γ are calculated by using various methods, e.g., the intermediate neglect of differential overlap for spectroscopy, the complete neglect of differential overlap for spectroscopy, and so on.[16–19] The results of the cal-

TABLE II. The observed and the calculated frequencies of Raman active and infrared active modes, expressed in cm^{-1}.

Raman active	Observed[a]	Calculated	Infrared active	Observed[b]	Calculated
$a_g(1)$	496	521	$t_{1u}(1)$	528	542
$a_g(2)$	1470	1374	$t_{1u}(2)$	577	614
$h_g(1)$	273	282	$t_{1u}(3)$	1183	1161
$h_g(2)$	437	413	$t_{1u}(4)$	1429	1376
$h_g(3)$	710	598			
$h_g(4)$	774	795			
$h_g(5)$	1099	1117			
$h_g(6)$	1250	1246			
$h_g(7)$	1428	1442			
$h_g(8)$	1575	1627			

[a]Reference 23.
[b]Reference 24.

culations generally show that the levels, $^1T_{1g}$, $^1T_{2g}$, and ^1G_g, are nearly degenerate within the energy interval of $\sim$0.1 eV, while the ^1H_g level settles over the others about 0.3 eV. However, the orderings of the energies of the levels, $^1T_{1g}$, $^1T_{2g}$, and ^1G_g, are altered depending on the methods of calculations. Therefore, we use two sets of E_Γ in order to examine the dependence of our results on E_Γ; one is calculated by Bendale, Baker, Zerner[18] and the other by Negri, Orlandi, and Zerbetta.[19] The values of E_Γ are listed in Table III.

Furthermore, we define the interaction energy, $E^\gamma_{\rm int}$, of the γ mode in the following way. First, we consider a simple model whose Hamiltonian is given by $|{\rm ex}\rangle(E_{\rm ex}-cQ)\langle{\rm ex}|+m\omega^2Q^2/2$ where Q is a mode interacting with an excited state, $|{\rm ex}\rangle$, and $E_{\rm ex}$ is the energy of $|{\rm ex}\rangle$. Then one easily finds that the energy of the excited state is lowered from $E_{\rm ex}$ by $-c^2/2m\omega^2$ in the relaxed configuration, $Q^*=c/m\omega^2$. That is, the energy gain due to the relaxation is given by $c^2/2m\omega^2$. This implies that the magnitude of the energy gain is that of the elastic energy itself. Therefore, it is natural to define $E^\gamma_{\rm int}$ by its contribution to the elastic energy in the relaxed configuration, u^*. That is, the elastic energy $E_{\rm elastic}(u^*)$ are decomposed into $E^\gamma_{\rm int}$ from each normal mode:

$$E_{\rm elastic}(u^*)=\sum_\gamma E^\gamma_{\rm int}\ , \tag{16}$$

where

$$E^\gamma_{\rm int}=\tfrac{1}{2}\sum_i m\omega^2_\gamma Q^{*2}_{\gamma i}\ . \tag{17}$$

Here $Q^*_{\gamma i}$ represents the displacement of the ith coordinate of the γ mode in the relaxed configuration.

Now we sketch the outline of the numerical calculations. The results are presented in the next section. Under a given atomic configuration u, the Hamiltonian (15) is diagonalized and then the lowest eigenvalue, $E_{\rm lowest}(u)$, is determined, which represents the adiabatic potential of the lowest excited state. By minimizing $E_{\rm lowest}(u)$ with respect to u, one finds the equilibrium configuration u^* and the energy of the relaxed excited state, $E_{\rm lowest}(u^*)$. Furthermore, by using $E^\gamma_{\rm int}$ defined in Eq. (17), we elucidate the vibrational modes enormously contributing to the Jahn-Teller distortion. Finally, the frequencies of the normal modes in the relaxed excited state are calculated by diagonalizing the Hessian, $\partial^2E_{\rm lowest}(u)/\partial u_\alpha\partial u_\beta|_{u=u^*}$.

TABLE III. The energies of the low-lying excited states derived from the quantum chemical calculations, expressed in eV.

Energy level	Bendale, Baker and Zerner[a]	Orlandi, Negri, and Zerbetto[b]
T_{1g}	2.11	2.33
T_{2g}	2.17	2.29
G_g	2.23	2.34
H_g	2.52	2.65

[a]Reference 18.
[b]Reference 19.

III. RESULTS AND DISCUSSION

We start with a group theoretical consideration. The molecular structure of C_{60} in the relaxed excited state differs from that in the ground state when there exists a nonvanishing $H^{\rm ep}_{\Gamma I,\Gamma' I'}(u)$ in the Hamiltonian. This occurs unless $V^{\rm ep}_{mm'}$ and $V^{\rm ep}_{aa'}$ in Eq. (11) are all zero, where $V^{\rm ep}_{mm'}$ and $V^{\rm ep}_{aa'}$ are the one-electron matrix elements of the electron-phonon interaction between LUMO (t_{1u}), m and m', and those between HOMO (h_u), a and a', respectively. Then the excited states couple with the normal mode whose representation appears in the symmetric representations, $[t_{1u}\times t_{1u}]$ and/or $[h_u\times h_u]$. Consequently, one finds that only a_g, g_g, and h_g modes are coupled with the excited states, i.e., $[t_{1u}\times t_{1u}]=a_g+h_g$ and $[h_u\times h_u]=a_g+g_g+2h_g$. In particular, it is expected that the h_g modes significantly contribute to the Jahn-Teller distortion.

In order to confirm the above consideration, we carry out the numerical calculations as explained in the last of Sec. II D. First, we elucidate the structure of the molecule in the relaxed excited state. At least, it is apparent that the structure is symmetrical under the space inversion because only even-parity modes can couple with the excited states. Actually, it is found that the symmetry of the relaxed structure is approximately C_{2h}, though the exact symmetry is C_i. In Fig. 1(a), we show the side view of the molecule in the relaxed excited state by illus-

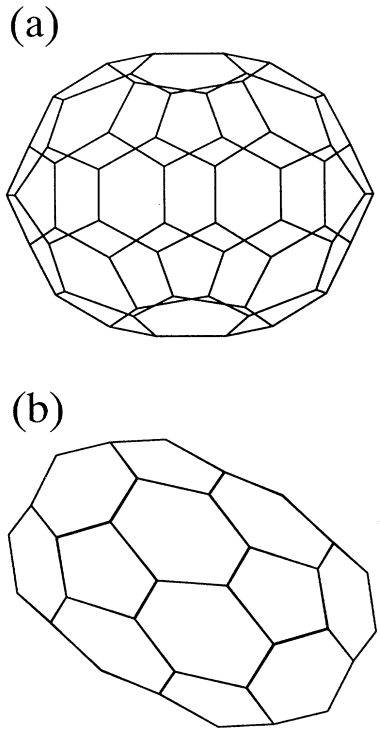

FIG. 1. (a) Side view and (b) top view of the C_{60} molecule in the relaxed excited state. The distortion is illustrated ten times the size of the actual one. The pseudotwofold axis penetrates the molecule vertically in (a) and is perpendicular to the figure in (b).

trating the distortion ten times the size of the actual one. The pseudotwofold axis penetrates the molecule vertically in Fig. 1(a). Also the top view is shown in Fig. 1(b) where the pseudotwofold axis is perpendicular to the figure. It appears that the symmetry of the relaxed structure is hardly distinguishable from C_{2h} in view of Figs. 1(a) and (b).

Next, in Table IV, we list the energy of the relaxed excited state, $E_{\rm lowest}(u^*)$, the elastic energy, $E_{\rm elastic}(u^*)$, and the relaxation energy, $E_{\rm relax}(u^*)$, which is defined by $E_{\rm lowest}(u^*)-E_{\rm lowest}(0)$; $E_{\rm lowest}(0)$ is the lowest of E_Γ. It should be noted that $E_{\rm lowest}(u^*)$ shows direct dependence on the lowest of E_Γ. Therefore, the two listed values of $E_{\rm lowest}(u^*)$ are somewhat different from each other because the lowest of E_Γ calculated by Bendale, Baker, and Zerner is $E_{T_{1g}}$=2.11 eV; on the other hand, that calculated by Negri, Orlandi, and Zerbetto is $E_{T_{2g}}$=2.29 eV. To the contrary, both $E_{\rm elastic}(u^*)$ and $E_{\rm relax}(u^*)$ are almost independent of the choice of E_Γ because they do not depend on the absolute values of E_Γ but only depend on the splittings between them.

Using the energies listed in Table IV, we estimate the energy of the absorption edge, $E_{\rm edge}$, and the peak energy of the luminescence, $E_{\rm peak}$; the observed values are $E_{\rm edge}=1.9$ eV and $E_{\rm peak}=1.7$ eV. One should remember that $E_{\rm edge}$ is $E_{\rm lowest}(u^*)$ itself (zero-phonon transition) and $E_{\rm peak}$ is given by $E_{\rm lowest}(u^*)-E_{\rm elastic}(u^*)$ (Franck-Condon transition), where we measure the energy of the excited state from the energy of the ground state. Then our results yield $E_{\rm edge}=1.70$ or 1.86 eV and $E_{\rm peak}=1.24$ or 1.40 eV, according to the choice of E_Γ in our calculations. Furthermore, the magnitude of the electron-phonon interaction is deduced from $E_{\rm edge}$ and $E_{\rm peak}$, i.e., $E_{\rm edge}-E_{\rm peak}$ which is nothing but $E_{\rm elastic}(u^*)$; this gives the measure of the magnitude of the electron-phonon interaction, as is explained in the last of Sec. II D. Therefore, it is found that the calculated results, $E_{\rm elastic}(u^*)=0.46$ eV, give the same order as the observed value, $E_{\rm edge}-E_{\rm peak}\sim$0.2 eV.[25]

Furthermore, we elucidate the vibrational modes enormously contributing to the Jahn-Teller distortion by decomposing the elastic energy $E_{\rm elastic}(u^*)$ into the parts from individual modes; the interaction energy of the γ mode is denoted by $E_{\rm int}^\gamma$ which is defined by Eq. (17). In Table V, we list $E_{\rm int}^\gamma$ of the a_g and the h_g modes, while those of the g_g modes are left out because it is found that all $E_{\rm int}^{g_g}$ are less than 0.0001 eV. Consequently, we find that the mode most significantly contributing to the Jahn-Teller distortion is the $h_g(1)$ mode ($E_{\rm int}^{h_g(1)}\cong 0.3$ eV) and the next is the $h_g(4)$ mode ($E_{\rm int}^{h_g(4)}\cong 0.1$ eV). One also finds that $E_{\rm int}^\gamma$ of the other modes are one or more orders of magnitude less than those of the $h_g(1)$ and the $h_g(4)$ mode.

TABLE IV. The energy of the lowest excited state $E_{\rm lowest}(u^*)$, the elastic energy $E_{\rm elastic}(u^*)$, and the relaxation energy $E_{\rm relax}(u^*)$ in the relaxed configuration, expressed in eV.

Energy	Value[a]	Value[b]
$E_{\rm lowest}(u^*)$	1.70	1.86
$E_{\rm elastic}(u^*)$	0.46	0.46
$E_{\rm relax}(u^*)$	-0.41	-0.43

[a]Obtained by using E_Γ due to Bendale, Baker, and Zerner.
[b]Obtained by using E_Γ due to Negri, Orlandi, and Zerbetto.

TABLE V. The interaction energy, $E_{\rm int}^\gamma$, of the a_g and the h_g modes, in eV.

Mode	$E_{\rm int}^{\gamma}$ [a]	$E_{\rm int}^{\gamma}$ [b]
$a_g(1)$	0.003	0.003
$a_g(2)$	0.003	0.003
$h_g(1)$	0.299	0.300
$h_g(2)$	0.017	0.017
$h_g(3)$	0.004	0.004
$h_g(4)$	0.113	0.113
$h_g(5)$	0.004	0.004
$h_g(6)$	0.013	0.013
$h_g(7)$	0.001	0.001
$h_g(8)$	0.001	0.001

[a]Obtained by using E_Γ due to Bendale, Baker, and Zerner.
[b]Obtained by using E_Γ due to Negri, Orlandi, and Zerbetto.

The interaction energies $E_{\rm int}^\gamma$ give important insight into the interaction between the vibrational modes and the excited states; however, they themselves are not the directly observable quantities. Then we present the results of the calculations on the frequencies of the normal modes in the relaxed excited state, which are the experimentally observable quantities. In Table VI, we list the calculated frequencies of the h_g modes in the ground state and those of the corresponding modes in the relaxed excited state where the frequencies are split due to the reduction of the symmetry of the molecular structure from I_h to C_i. We find that the frequency shifts of the $h_g(1)$ and the $h_g(4)$ mode reach several tens of $\rm cm^{-1}$. It is most likely that this indicates the extraordinary contributions of the $h_g(1)$ and the $h_g(4)$ mode to the Jahn-Teller distortion. That is, we again conclude that the $h_g(1)$ and the $h_g(4)$ mode are very strongly coupled with the low-lying excited states, as is mentioned in the preceding paragraph. Also, it is found that the shifts in the frequencies of the other modes are all less than 1 $\rm cm^{-1}$, so that we omit them from Table VI.

Next we specify the characteristics of the $h_g(1)$ and the $h_g(4)$ mode. To this end, we make a very simple approximation where the C_{60} molecule is regarded as the sphere made up of a thin film. Then one needs three sets of spherical harmonics as the complete system to describe the vibrational motions of the sphere because each infinitesimal element of the sphere surface has three degrees of freedom; one represents the radial motions and the other two the tangential ones. They are known as vector spherical harmonics:[26]

$$\mathbf{X}_{lm}^{\rm r}(\hat{\mathbf{r}})=\hat{\mathbf{r}}Y_{lm}(\hat{\mathbf{r}})\ , \tag{18}$$

$$\mathbf{X}_{lm}^{\rm t+}(\hat{\mathbf{r}})=\frac{r\nabla Y_{lm}(\hat{\mathbf{r}})}{\sqrt{l(l+1)}}\ , \tag{19}$$

TABLE VI. The calculated frequencies of the normal modes in the ground state and those in the relaxed excited state, expressed in cm^{-1}.

Mode	Calculated frequencies in the ground state		Calculated frequencies[a] in the relaxed excited state			
$h_g(1)$	282	208	243	274	274	281
$h_g(2)$	413	403	408	413	413	413
$h_g(3)$	598	584	589	596	596	598
$h_g(4)$	795	756	765	783	790	794
$h_g(5)$	1117	1112	1112	1114	1115	1117
$h_g(6)$	1246	1229	1236	1244	1245	1246
$h_g(7)$	1442	1431	1437	1439	1441	1442
$h_g(8)$	1627	1624	1624	1626	1626	1627

Mode	Calculated frequencies in the ground state		Calculated frequencies[b] in the relaxed excited state			
$h_g(1)$	282	198	242	273	274	281
$h_g(2)$	413	402	407	413	413	413
$h_g(3)$	598	583	589	595	596	598
$h_g(4)$	795	752	764	782	790	794
$h_g(5)$	1117	1112	1112	1114	1115	1117
$h_g(6)$	1246	1228	1235	1244	1245	1246
$h_g(7)$	1442	1430	1436	1439	1441	1442
$h_g(8)$	1627	1624	1624	1626	1626	1627

[a]Obtained by using E_Γ due to Bendale, Baker, and Zerner.
[b]Obtained by using E_Γ due to Negri, Orlandi, and Zerbetto.

and

$$\mathbf{X}^{t-}_{lm}(\hat{\mathbf{r}}) = \frac{-i\mathbf{r}\times\nabla Y_{lm}(\hat{\mathbf{r}})}{\sqrt{l(l+1)}} . \tag{20}$$

Here $Y_{lm}(\hat{\mathbf{r}})$ is the usual spherical harmonics. $\mathbf{X}^{r}_{lm}(\hat{\mathbf{r}})$ and $\mathbf{X}^{t\pm}_{lm}(\hat{\mathbf{r}})$ describe the radial and the tangential motions, respectively. Then the normal modes of the molecule are classified by the order of spherical harmonics, l. Also, it will be shown that the parity of $\mathbf{X}^{r}_{lm}(\hat{\mathbf{r}})$, $\mathbf{X}^{t+}_{lm}(\hat{\mathbf{r}})$, and $\mathbf{X}^{t-}_{lm}(\hat{\mathbf{r}})$ are $(-1)^l$, $(-1)^l$, and $(-1)^{l+1}$, respectively. Therefore, there are two even and one odd normal mode when l is even but one even and two odd normal modes when l is odd.

In describing the h modes (h_g and h_u) by using the vector spherical harmonics, it is necessary to use those of five distinct l because the total number of the h modes is 15. Then, by reducing the irreducible representations of the rotation group to those of I_h, one finds that the h representation arises from $l = 2,4,5,6,7$ when five l are picked up from the lowest ($l = 2$). As a result, there arise three radial ($l = 2,4,6$) and five tangential ($l = 2,4,5,6,7$) h_g modes; the h_g modes whose l are odd ($l = 5,7$) are described by $\mathbf{X}^{t-}_{lm}(\hat{\mathbf{r}})$. On the other hand, it is well known that the three h_g modes of lower frequencies, $h_g(1)$, $h_g(2)$, and $h_g(3)$, are the radial modes, while the other five h_g modes of the higher frequencies are the tangential ones.[27] Therefore, it is natural to consider that the radial h_g mode of the lowest frequency, $h_g(1)$, is well described by $\mathbf{X}^{r}_{lm}(\hat{\mathbf{r}})$ of $l = 2$ and the tangential one of the lowest frequency, $h_g(4)$, by $\mathbf{X}^{t+}_{lm}(\hat{\mathbf{r}})$ of $l = 2$. That is, the $h_g(1)$ and the $h_g(4)$ mode are the radial and the tangential h_g mode of $l = 2$, respectively.

In Table VII, we list the average of the squares of the radial displacements of the carbon nuclei, $\langle u_r^2\rangle$, and that of the tangential ones, $\langle u_t^2\rangle$, of the h_g modes. The results clearly show that three h_g modes of lower frequencies are the radial modes while the five of higher frequencies are the tangential ones. Moreover, it should be noted that the $h_g(1)$ mode is 75% radial and 25% tangential while the $h_g(4)$ mode is 25% radial and 75% tangential. Such complementary ratios of the radial and the tangential components also indicate that the $h_g(1)$ and the $h_g(4)$ mode belong to the same l. That is, it is most likely that the $h_g(1)$ and the $h_g(4)$ mode are caused by the moderate mixing of $\mathbf{X}^{r}_{lm}(\hat{\mathbf{r}})$ and $\mathbf{X}^{t+}_{lm}(\hat{\mathbf{r}})$ of $l = 2$. Furthermore, we present more direct evidence of our proposition that both the $h_g(1)$ and the $h_g(4)$ mode belong to $l = 2$. Since the number of the nodal lines of $Y_{lm}(\hat{\mathbf{r}})$ is equal to l, one can find the primarily contributing l to an individual mode

TABLE VII. The average of the squares of the radial displacements, $\langle u_r^2\rangle$, and that of the tangential one, $\langle u_t^2\rangle$, of the h_g modes.

Mode	$\langle u_r^2\rangle$	$\langle u_t^2\rangle$
$h_g(1)$	0.746	0.254
$h_g(2)$	0.978	0.022
$h_g(3)$	0.987	0.013
$h_g(4)$	0.246	0.754
$h_g(5)$	0.007	0.993
$h_g(6)$	0.012	0.988
$h_g(7)$	0.014	0.986
$h_g(8)$	0.010	0.990

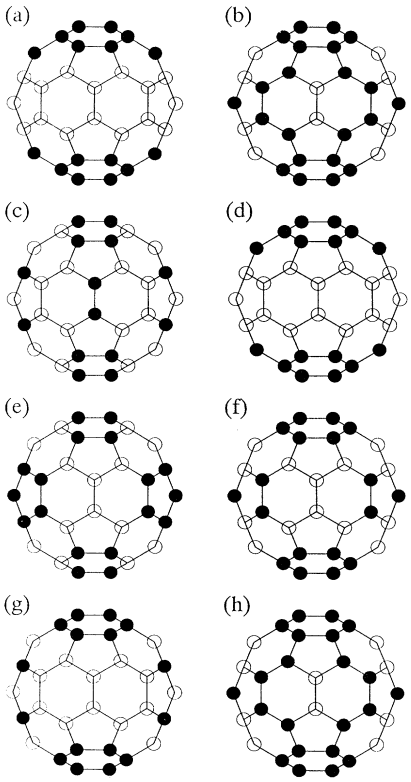

FIG. 2. Vibrational pattern of the radial displacements of the carbon nuclei. (a) $h_g(1)$, (b) $h_g(2)$, (c) $h_g(3)$, (d) $h_g(4)$, (e) $h_g(5)$, (f) $h_g(6)$, (g) $h_g(7)$, and (h) $h_g(8)$. The open and the closed circles represent the outward and the inward displacements of the carbon nuclei, respectively.

by illustrating the vibrational pattern of the radial displacements. The results are shown in Figs. 2(a)–2(h), where the open and the closed circles represent the outward and the inward displacements of the carbon nuclei, respectively; in this figure, we show the patterns of the modes which have the same symmetry as one of the basis functions of h_g representation, $2z^2 - x^2 - y^2$. It is found that two nodal lines clearly appear in the patterns of both the $h_g(1)$ and the $h_g(4)$ mode, i.e., they belong to $l = 2$.

Finally, we refer to the accuracy of the present results. First, we examine the effects of the exploited value of the dielectric constant, $\epsilon = 6$, in Eq. (7). The dielectric constant appears in the denominator of the electron-phonon interaction $H^{\rm ep}_{\Gamma I,\Gamma' I'}(u)$ in the Hamiltonian, so that one will find that $E_{\rm elastic}(u^*)$ are approximately proportional to ϵ^{-2}, remembering the simple consideration given in Sec. II D. Therefore, it is expected that the quantities related to $E_{\rm elastic}(u^*)$ show the same dependence on ϵ, for example, the interaction energy $E^{\gamma}_{\rm int}$ and the splittings of the vibrational frequencies in the relaxed excited state. It should be noted, however, that the magnitude of such quantities is preserved within the same order as is obtained in the present study as long as ϵ remains in the range of 4–8. Next, we note that our results depend on the one-electron wave functions $\phi_i(\mathbf{r})$ in Eq. (10) which are obtained by using the first-principle method. Although the exploited basis set is a minimal one, it is most likely that the qualitative features of our results are unchanged even if one uses a larger basis set because the method of the calculations is the same in the sense that it is the first-principle one. Furthermore, we perform the present calculations by using two sets of the energies of the unrelaxed excited states, E_Γ, which are obtained by the quantum chemical calculations. It is found, however, that our results are almost independent of the choice of E_Γ.

IV. CONCLUSIONS

We study several properties of the lowest excited singlet state of the C_{60} molecule in connection with the Jahn-Teller distortion. The model Hamiltonian is employed in order to describe the electron-phonon interaction between the low-lying excited singlet states and the deformation of the C_{60} molecule. In the Hamiltonian, we exploit the force-constant model to represent the elastic property of the molecule, which reproduces the observed frequencies of the normal modes. Also the matrix elements of the electron-phonon interaction are calculated by using the one-electron wave functions obtained by the first-principle method. The relaxed excited state is determined by minimizing the lowest eigenvalue of the Hamiltonian with respect to the atomic configuration. The results of the calculations show that the symmetry of the molecular structure in the relaxed excited state is approximately C_{2h}, though the exact symmetry is C_i. Also we explore the vibrational modes significantly contributing to the Jahn-Teller distortion. As a result, it is found that the $h_g(1)$ and the $h_g(4)$ modes are the most and the next most crucial mode, respectively. Furthermore, we calculate the frequencies of the normal modes in the relaxed excited state and then find that the splittings of the frequencies of the $h_g(1)$ and the $h_g(4)$ modes reach several tens of $\rm cm^{-1}$. Finally, it is pointed out that the $h_g(1)$ and the $h_g(4)$ modes are the radial and the tangential modes of $l = 2$, respectively.

ACKNOWLEDGMENTS

We would like to thank M. Fujita for helpful discussions. One of the authors (S.S.) is grateful to Y. Iwasa for valuable discussions.

[1] N. Minami, Chem. Lett. **238**, 1791 (1991).
[2] N. Minami, Mol. Cryst. Liq. Cryst. **217**, 231 (1992).
[3] Y. Wang and L. T. Cheng, J. Phys. Chem. **96**, 1530 (1992).
[4] S. R. Flom, R. G. S. Pong, F. J. Bartoli, and Z. H. Kafafi, Phys. Rev. B **46**, 15 598 (1992).
[5] W. Krätschmer, L. D. Lamb, K. Fostiropoulos, and D. R. Huffman, Nature (London) **347**, 354 (1990).
[6] H. Ajie, M. M. Alvarez, S. J. Anz, R. D. Beck, F. Diederich,

K. Fostiropoulos, D. R. Huffman, W. Krätschmer, Y. Rubin, K. E. Shriver, D. Sensharma, and R. L. Whetten, J. Phys. Chem. **94**, 8630 (1990).
[7]J. P. Hare, H. W. Kroto, and R. Taylor, Chem. Phys. Lett. **177**, 394 (1991).
[8]J. B. Howard, J. T. McKinnon, Y. Makarovsky, A. L. Lafleur, and M. E. Johnson, Nature (London) **352**, 139 (1991).
[9]M. K. Kelly, P. Etchegoin, D. Fuchs, W. Krätschmer, and K. Fostiropoulos, Phys. Rev. B **46**, 4963 (1992).
[10]S. Leach, M. Vervloet, A. Desprès, E. Bréheret, J. P. Hare, T. J. Dennis, H. W. Kroto, R. Taylor, and D. R. M. Walton, Chem. Phys. **160**, 451 (1992).
[11]C. Reber, L. Yee, J. McKiernan, J. I. Zink, R. S. Williams, W. M. Tong, D. A. A. Ohlberg, R. L. Whetten, and F. Diederich, J. Phys. Chem. **95**, 2127 (1991).
[12]S. P. Sibley, S. M. Argentine, and A. H. Francis, Chem. Phys. Lett. **188**, 187 (1992).
[13]P. A. Lane, L. S. Swanson, Q.-X. Ni, J. Shinar, J. P. Engel, T. J. Barton, and L. Jones, Phys. Rev. Lett. **68**, 887 (1992).
[14]Y. Wang, J. Phys. Chem. **96**, 764 (1992).
[15]M. Matus, H. Kuzmany, and E. Sohmen, Phys. Rev. Lett. **68**, 2822 (1992).
[16]I. László and L. Udvardi, Chem. Phys. Lett. **136**, 418 (1987).
[17]F. Negri, G. Orlandi, and F. Zerbetto, Chem. Phys. Lett. **144**, 31 (1988).
[18]R. D. Bendale, J. D. Baker, and M. C. Zerner, Int. J. Quantum Chem. Symp. **25**, 557 (1991).
[19]F. Negri, G. Orlandi, and F. Zerbetto, J. Chem. Phys. **97**, 6496 (1992).
[20]Y. Toyozawa, Prog. Theor. Phys. **20**, 53 (1958).
[21]R. L. Disch and J. M. Schulman, Chem. Phys. Lett. **125**, 465 (1986).
[22]K. Hedberg, L. Hedberg, D. S. Bethune, C. A. Brown, H. C. Dorn, R. D. Johnson, and M. de Vries, Science **254**, 410 (1991).
[23]D. S. Bethune, G. Meijer, W. C. Tong, H. J. Rosen, W. G. Golden, H. Seki, C. A. Brown, and M. S. Derries, Chem. Phys. Lett. **179**, 181 (1991).
[24]W. Krätschmer, K. Fostiropoulos, and D. R. Huffman, Chem. Phys. Lett. **170**, 167 (1990).
[25]We assume that only even-parity modes relating to the Jahn-Teller distortion dominantly affect the optical processes. It should be noted, however, that there is another interpretation about the vibrational structures in the optical spectra; several authors suggest that the odd-parity modes are crucial for the explanation of the vibrational structures in the spectra. For example, see Ref. 19.
[26]M. E. Rose, *Elementary Theory of Angular Momentum* (Wiley, New York, 1957).
[27]R. E. Stanton and M. D. Newton, J. Phys. Chem. **92**, 2141 (1988).